Robust Data-Partitioned Video Streaming over a WiMAX Channel

Laith Al-Jobouri, Martin Fleury, and Mohammed Ghanbari
School of Computer Science and Electronic Engineering
University of Essex, Colchester, United Kingdom
{lamoha, fleum, ghan}@essex.ac.uk

***Abstract*—This paper demonstrates a robust layered video scheme, based on data-partitioning and intended for IPTV streaming over wireless broadband. Equal error protection through rateless coding is applied, whereby higher-priority data partitioned packets are protected by appropriate selection of quantization parameter and picture slicing, so as to regulate packet size. In the mobile WiMAX channel investigated, both packet drops from congestion and adverse channel conditions are shown to be affected by packet size. The main proposal is for adaptive rateless coding in which additional redundant data are retransmitted to heal corrupted packets. However, though these packets are always repairable, delay increases as the percentage of corrupted packets increases, affecting the design parameters. Intra-refresh macro blocks are added to prevent the objective video quality falling below an acceptable level. Picture slicing further reduces the packet size to increase robustness in the face of measurement noise during channel estimation and the effects of slow and fast fading.**

Keywords- data-partitioning; IPTV; layered source coding; rateless channel coding; WiMAX

I. INTRODUCTION

Data-partitioned (DP) [1] video streaming is a form of layered coding [2], which lacks the complexity and data dependencies of scalable video coding (SVC). This paper considers ways of improving the robustness of DP streaming in the context of IPTV over a broadband wireless channel. IPTV provides video streaming through video-on-demand (VoD) and time-shifted TV, the popularity of which has been demonstrated in the UK by the BBC's iPlayer [3]. Multicast varieties of video streaming such as near-VoD and broadcast TV are also on the horizon. The BBC iPlayer uses a simple form of simulcast to cope with differing asymmetric digital subscriber line bandwidth capacities. However, this form of scalability may be insufficient to cope with channel variability from fading in mobile broadband channels [4] as, for example, presented by IEEE 802.16e (mobile WiMAX) [5].

Though it has been suggested that the SVC extension to the H.264/AVC (Advanced Video Coding) standard codec is suitable for wireless IPTV [6], the dependencies of enhancement layer data on key picture data within the base layer may require extra transmission protection. These dependencies were introduced to avoid the overhead of fine-grained scalability in the earlier MPEG-4 codec. DP video in contrast has just three layers with only the highest priority H.264/AVC partition-A bearing packets being vital to reconstruction of a picture.

However, a key issue remaining for DP streaming is how to provide protection against a harsh channel environment. For example, this paper considers outright packet drops through burst errors due to a mobile device entering a deep fade caused by a change of wireless environment. In this situation, a packet either fails to pass the signal strength threshold at the receiver or fails to pass checksum tests at the transport level. Consequently, the packet is dropped before ever reaching application layer software. The paper also considers packets that are corrupted but may still be repairable by Forward Error Correction (FEC) and consequentially are passed from the transport layer up the protocol stack to the application layer. This is possible if UDP-lite [7] rather than UDP is employed for streaming, as UDP-lite provides partial checksums. The paper considers error bursts at the byte-level as a source of corrupted packets, as may arise from fast fading due to multipath reception.

To provide protection, adaptive FEC through the agency of rateless channel codes [8] avoids the main weakness of FEC, a constant overhead even when the channel conditions are temporarily benign. To achieve this, the channel conditions giving rise to corrupted packets are estimated in a conservative manner that accounts for possible measurement noise. However, this does not account for dropped packets both from channel conditions and possible sending buffer overflow. In this paper, the latter threat receives a partial remedy in the form of smaller packet sizes for higher priority packets, as this is a way of reducing the effects of congestion *and* channel conditions. Smaller packets for higher priority packets are a natural consequence of DP video. However, the packets can be made still smaller by slicing pictures so that DP video packets occur within each of several slices. The main potential weakness of the scheme is that with smaller packets, the overhead from headers increases. One way to ameliorate the impact of header overhead is through header compression, which can achieve up to 97.5% compression [9] for the IPv4/UDP/Real Time Protocol (RTP) combination, but certainly this issue deserves further consideration. We are

also aware that unequal error protection such as arises from hierarchical modulation in [10] is available as an alternative solution for the protection of higher priority DP video but in this paper, a packetization solution is considered and equal error protection is applied. It is not claimed that equal error protection is better than unequal error protection but that it can achieve satisfactory results provided due attention is paid to ensuring high-priority data is carried in smaller packets. Equal error protection can also avoid the implementation costs of unequal error protection, either in terms of physical layer modifications [10] or in the need for application-specific cross-layer intervention. It should be noted that for very noisy channels the increase in redundant data may be prohibitive, as the goodput or effective throughput will be severely reduced. However, in these circumstances redundant partition-A packets can be sent along with the original data stream. Space does not allow presentation of our redundant partition packet scheme in this paper.

Finally, to further improve robustness, intra-refresh macroblocks (MBs) [11] rather than periodic refresh pictures are employed. This provision avoids the high data rate spikes of intra-coded I-pictures and is suitable for iPlayer-like services, though without adaptation is not suitable for multicast varieties of IPTV with channel swapping. However, the inclusion of intra-refresh MBs does lead to some increase in the size of H.264/AVC partition-B bearing packets.

The H.264/AVC codec increases the compression ratio of Digital Video Broadcasting (DVB)'s MPEG-2 codec by as much as 50% [12], which is why it is of interest to IPTV transmission over bandwidth-limited wireless channels. H.264/AVC, as part of its network-friendly approach, introduces Network Abstraction Layer units (NALUs) as a per-slice container for transmission. Data partitioning of NALUs into partition-A, -B, and -C types of decreasing importance for decoder reconstruction purposes normally results in Real Time Protocol (RTP) packets of increasing size. This is achieved by setting the variable-bit-rate video's quantization parameter (QP) in such a way that lower-priority texture data, which can be compensated for more easily at the decoder, occupies a larger proportion of a video frame's compressed data. Consequently, when partition-C data are packetized in a WiMAX Medium Access Control (MAC) Service Data Unit (MSDU) within a MAC Protocol Data Unit (MPDU), the longer packet is more likely to suffer error than MSDUs bearing data from other partitions. However, the decoder can apply motion copy error concealment to reconstruct missing partition-C data by means of the motion vectors still available in partition-A.

The next Section of this paper now describes in more detail the source and channel coding concepts employed in this paper.

Table I. NAL unit types

NAL unit type	Class	Content of NALU
0	-	Unspecified
1	VCL	Coded slice
2	VCL	Coded slice partition A
3	VCL	Coded slice partition B
4	VCL	Coded slice partition C
5	VCL	Coded slice of an IDR picture
6-12	Non-VCL	Suppl. info., Parameter sets, etc.
13-23	-	Reserved
24-31	-	Unspecified

II. CONTEXT

A. *Data-partitioning*

The H.264/AVC codec conceptually separates the Video Coding Layer (VCL) from the Network Abstraction Layer (NAL). The VCL specifies the core compression features, while the Network Adaptation Layer (NAL) facilitates the delivery of the H.264 VCL data to the underlying transport layers such as IP/UDP/RTP, H.32X and MPEG-2 transport system. In this paper, IP/UDP/RTP is assumed. Each NALU could be considered as a packet that contains a header and a payload. The header specifies the NALU type and the payload contains the related data. Table I is a summarized list of different NALU types. NALUs 6 to 12 are non-VCL units containing additional information such as parameter sets and supplemental information.

In H.264/AVC, when data-partitioning is enabled, every slice is divided into three separate partitions and each partition is located in either of type 2 to type-4 NALUs, as listed in Table I. NALU of type 2, also known as partition-A comprises the most important information of the compressed video bit-stream of P- and B-pictures (when present), including the MB addresses, motion vectors (MVs) and essential headers. If any MBs in these pictures are intra-coded, their Discrete Cosine Transform (DCT) coefficients are packed into a type-3 NALU, also known as partition-B. There are two types of intra-coded MBs: those that are naturally encoded as the result of a decision by the encoder and those that are added because intra-coded refresh is activated, as occurs in this paper. SKIP MBs also occur when an encoder decides that a direct copy of a previous frame's MB can be made.

Type 4 NAL, also known as partition-C, carries the DCT coefficients of the motion-compensated inter-picture coded MBs. As in I-slices all MBs are spatially encoded, type 5 NALUs are very long. On the other hand A and B partitions of data-partitioned P- and B-slices (when present) are smaller but their C-type partition can be very long.

Fig. 1 is a comparison between the relative sizes of the partitions according to QP for the video clip which is employed in Section V's evaluation. The test sequence was *Football*, which is a reference video clip with high motion. *Football* was Variable Bit Rate (VBR) encoded at Common Intermediate Format (CIF) (352×288 pixel/frame), with a

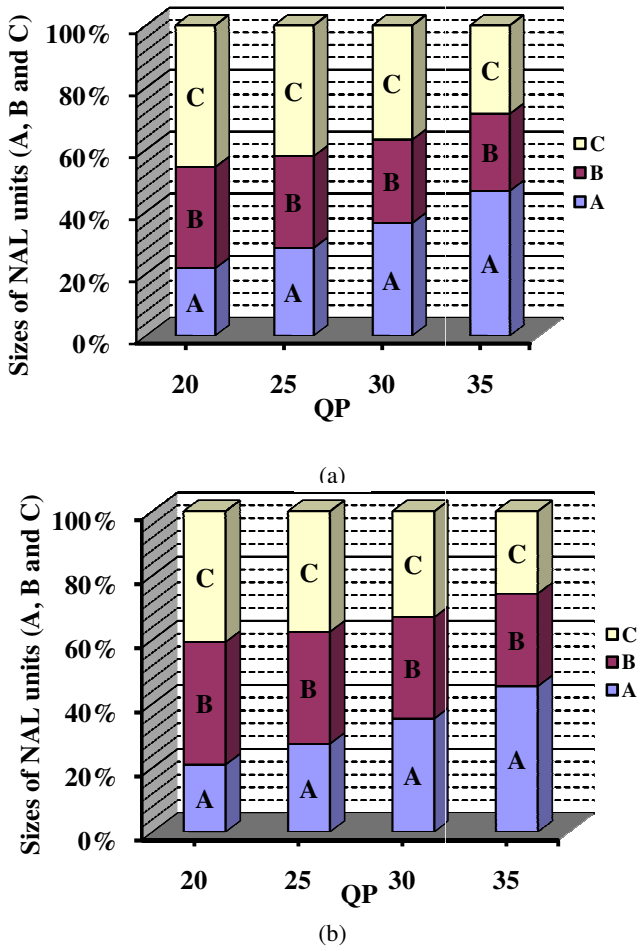

Figure 1. Relative sizes of data partitions according to quantization paramater (QP) for the *Football* video sequence, with (a) 5% intra-coded refresh MBs, and (b) 25% intra-coded refresh MBs.

Group of Pictures (GOP) structure of IPPP….. at 30 frame/s, i.e. one initial I-picture followed by all predictive P-pictures. This arrangement removes the complexity of bi-predictive B-frames at a cost in increased bit rate.

In H.264/AVC, the QP range is from 0 to 51, with a low QP representing high quality. From the Figure it is apparent that partition-B's contribution increases as the percentage of intra-refresh macroblocks is increased, making partition-B packets more vulnerable to congestion and channel error as a result. The size of partition-C bearing packets declines with increasing QP as a result of coarser quantization of DCT coefficients.

Table II reports the absolute partition NALU sizes. It might be thought that partition-A's size would be unaffected by change of QP. However, as H.264/AVC uses variable block size motion compensation, the number of MVs per MB changes and, as higher QPs result in larger blocks, the size of partition-A reduces. For higher QP, a number of SKIP MBs may also be replaced by intra-refresh MBs, causing an increase in the size of partition-A. SKIP MBs are

Table II. NALU sizes with different Intra-Refresh amounts for the Football sequence.

	Average NALU size of Intra Refresh MB 5% (byte)			*Average NALU size of Intra Refresh MB 25% (byte)*		
QP	A	B	C	A	B	C
10	1845	2767	3867	1893	3450	3669
15	1690	1763	2511	1746	2216	2379
20	1463	1082	1482	1505	1346	1405
25	1120	595	682	1146	729	646

more common in static areas of a picture, and experiments with a sequence with more motion indicated that the partition-A anomaly reduced for such a sequence. The size of partition-A also increases for lower QPs if 25% intra-refresh MB is applied. This is because a greater mix of inter- and intra-coded MBs can also cause the block size to be varied. The dynamic range of the residual can also increase, resulting in larger partition-Cs.

Therefore, it is preferable to reduce the percentage of intra-refresh MBs, if this is possible without sacrificing robustness, in the interests of lower data-rates and lower packet sizes for the more important partitions A and B. The relatively small size of the A- and B-partitions is a potential advantage at low QPs but this comes at a cost of a high bitrate. Conversely, at the low quality end of the QP range, partition-A NALUs become relatively vulnerable to packet loss by virtue of their relatively increased length. Though there are some rules of thumb in analyzing the data-partioned NALU sizes and their relative proportions, the coding complexity of the H.264/AVC makes it difficult to develop firm rules. Besides, there is a variation with content type (such as the extent of motion) that space does not permit analysis of herein.

B. Rateless coding

Rateless channel coding allows the code rate to be adaptively changed according to channel conditions, avoiding the thresholding effect associated with fixed-rate codes such as Reed-Solomon (RS). This possibility allows the FEC overhead to be varied according to channel conditions.

A fixed-rate (n, k) RS channel code over an alphabet of size $q = 2^L$ has the property that if *any* k out of the n symbols transmitted are received successfully then the original k symbols can be decoded. However, for RS coding not only must n, k, and q be small but also the computational complexity of the decoder is of order $n(n - k) \log_2 n$. The error rate must also be estimated in advance.

In contrast, the class of Fountain codes [8] allows a continual stream of additional symbols to be generated in the event that the original symbols could not be decoded. It is the ability to easily generate new symbols that makes Fountain codes rateless. Decoding will succeed with small probability of failure if any of k $(1 + \varepsilon)$ symbols are successfully received. ε is the amount of additional

redundant data, expressed as a fraction of k, the number of information symbols. ε is related through k to the probability of decoder failure (as expressed later in this paragraph). Therefore, ε can be calculated according to a desired probability of decoder failure. In its simplest form, the symbols are combined in an exclusive OR (XOR) operation according to the order specified by a random low density generator matrix and in this case, the probability of decoder failure is $\partial = 2^{-k\varepsilon}$, which for large k approaches the Shannon limit. The random sequence must be known to the receiver but this is easily achieved through knowledge of the sequence seed.

Luby Transform (LT) codes reduce the complexity of decoding a simple Fountain code (which is of order k^3) by means of an iterative decoding procedure, provided that the column entries of the generator matrix are selected from a robust Soliton distribution. In the LT generator matrix case, the expected number of degree one combinations (no XORing of symbols) is $S = c \log_e(k/\partial)\sqrt{k}$, for small constant c. Setting $\varepsilon = 2 \log_e(S/\partial)\ S$ ensures that by sending $k(1 + \varepsilon)$ symbols these are decoded with probability $(1 - \partial)$ and decoding complexity of order $k \log_e k$.

If packets are pre-encoded with an inner code, a weakened LT transform can be applied to the symbols and their redundant symbols. The advantage of this Raptor code [13] is a decoding complexity that is linear in k. A systematic Raptor code is arrived at [13] by first applying the inverse of the inner code to the first k symbols before the outer pre-coding step.

III. SIMULATION MODEL

A. Rateless coding evaluation

In order to model Raptor coding, we employed the following statistical model [14]:

$$P_f(m,k) = 1 \quad \text{if } m < k,$$
$$= 0.85 \times 0.567^{\,m-k} \text{ if } m \geq k \qquad (1)$$

where $P_f(m,k)$ is the failure probability of the code with k source symbols if m symbols have been received. The authors of [14] remark and show that for $k > 200$ the model almost perfectly models the performance of the code.

The symbol size was set to bytes within a packet. Clearly, if instead 200 packets are accumulated before the rateless decoder can be applied (or at least equation (1) is relevant) there is a penalty in start-up delay for the video streaming and a cost in providing sufficient buffering at the mobile stations. In the experiments reported in this paper, the percentage redundancy for the Raptor code was adapted at the sender according to an estimate of the channel conditions. How this was done is reported in Section IV.

A corrupt packet can be detected by the Cyclic Redundancy Check (CRC) that is an optional part of the MPDU (WiMAX packet), refer to Fig. 2. Though this CRC

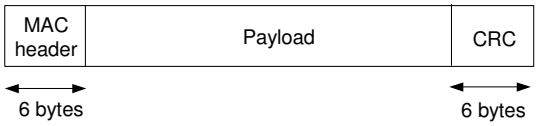

Figure 2. General format of a MAC PDU with optional CRC.

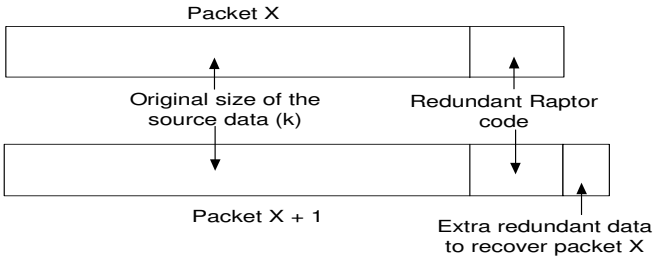

Figure 3. Division of payload data in a packet (MPDU) between source data, original redundant data and piggybacked data for a previous erroroneous packet.

also applies to the 4-byte MAC header, it does indicate the likelihood that a packet's payload is corrupt. Then, through measurement of channel conditions, an estimate of the number of symbols successfully received is made, giving a value m'. This implies from (1) that if less than k symbols (bytes) in the payload are successfully received then $k-m'+4$ redundant bytes can be sent to reduce the risk of failure to below 9%. Clearly, it is possible to improve the failure risk by simply including more bytes. However, in this paper we confine repeat transmissions of redundant bytes to a minimal amount, as we have found that video quality remains good. Future work will explore the effect on video quality of increasing the amount of extra redundant data retransmitted versus the delay that results.

To reduce latency, the number of retransmissions, after an Automatic Repeat Request (ARQ) over the uplink, was limited to one. The effect of this decision can be judged by the results in Section V. Recall that video is a real-time service and that further retransmissions risk missing picture display deadlines. Moreover, the possibility of interactive video applications such as videophone means that delay is normally minimized along the whole of the transmission path, including the WiMAX portion. Fig. 3 shows how ARQ triggered retransmissions work. In the Figure, packet X is corrupted to such an extent that it cannot be reconstructed. Therefore, in packet X+1 some extra redundant data is included up to the level that its failure is no longer certain. If the extra redundant data is insufficient to reconstruct the original packet, the packet is simply dropped. Otherwise, of course, it is passed to the H.264/AVC decoder.

B. Channel model

To establish the behavior of rateless coding under WiMAX the well-known ns-2 simulator augmented with a module from the Change Gung University, Taiwan [15] that

Table III. IEEE 802.16e parameter settings.

Parameter	*Value*
PHY	OFDMA
Frequency band	5 GHz
Bandwidth capacity	10 MHz
Duplexing mode	TDD
Frame length	5 ms
Max. packet length	1024 B
Raw data rate	10.67 Mbps
IFFT size	1024
Modulation	16-QAM 1/2
Guard band ratio	1/8
Channel model	Gilbert-Elliott
MS transmit power	245 mW
BS transmit power	20 W
Approx. range to SS	1 km
Antenna type	Omni-directional
Antenna gains	0 dBD
MS antenna height	1.2 m
BS antenna height	30 m

OFDMA = Orthogonal Frequency Division Multiple Access, QAM = Quadrature Amplitude Modulation, TDD = Time Division Duplex SS=subscriber station

has proved an effective way of modeling IEEE 802.16e's behavior.

We introduced a two-state Gilbert-Elliott channel model [16] in the physical layer of the simulation to simulate the channel model for WiMAX. To model the effect of slow fading at the packet-level, the PGG

(probability of staying in a good state) was set to 0.96, PBB (probability of staying in a bad state) = 0.95, PG (probability of packet loss in a good state) = 0.01 and PB (probability of packet loss in a bad state) = 0.02 for the Gilbert-Elliott parameters. Notice that PGB (probability of leaving the good state) is 1 – PGG, and similarly PBG = 1-PBB. Additionally, as mentioned in Section I, it is still possible for a packet not to be dropped in the channel but nonetheless to be corrupted through the effect of fast fading (or other sources of noise and interference). This byte-level corruption was modeled by a second Gilbert-Elliott model, with the same parameters (applied at the byte level) as that of the packet-level model except that PB (now probability of byte loss) was increased to 0.165.

C. WiMAX configuration

The physical layer (PHY) settings selected for WiMAX simulation are given in Table III. The antenna is modeled for comparison purposes as a half-wavelength dipole. The Time Division Duplex (TDD) frame length was set to 5 ms in experiments as it appears that this is the only setting specified by the WiMAX Forum, though the IEEE 802.16e standard allows for a range of settings. Setting to a lower value in the range (from 2.5 to 20 ms in the Standard) does not benefit real-time applications, as it limits the data that can be removed in any polling instance of a mobile station.

Video was transmitted over the downlink with UDP-lite transport. In order to introduce sources of traffic congestion, an always available FTP source was introduced with TCP transport to the SS. Likewise a Constant Bit Rate (CBR) source with packet size of 1000 B and inter-packet gap of 0.03 s was downloaded to the SS. While the CBR and FTP occupy the non-rtPS (non-real-time polling service) queue, rather than the rtPS queue, they still contribute to packet drops in the rtPS queue for the video, if the 50 packet rtPS buffer is already full or nearly full, while the nrtPS queue is being serviced.

D. Video configuration

The *Football* sequence, mentioned in Section II.A was employed for WiMAX channel downlink tests. Thus, *Football* with 260 CIF frames was VBR encoded at 30 frame/s. As a GOP structure of IPPP.... was employed, it is necessary to protect against error propagation in the event of inter-coded P-frame slices being lost. To ensure higher quality video, 5% intra-coded MBs (randomly placed) were included in each picture (apart for the first I-picture) to act as anchor points in the event of slice loss. Random placement of intra-refresh MBs allows the effect of differing proportions of such MBs to be judged. Cyclic intra-refresh lines [11] are a way of improving video quality because each picture sequence is guaranteed to be completely refreshed after a given number of pictures (18 for CIF).

At the decoder, motion copy error concealment was set, allowing the motion vectors contained in partition-A packets to indicate suitable replacement MBs within the last correctly received slice. The JM 14.2 version of the H.264/AVC codec software was employed with the Evalvid environment [17] used to reconstruct sequences according to reported packet loss from the simulator.

IV. ADAPTIVE RATELESS SCHEME

Three types of erroneous packets were considered: 1) packet drops at the BS sender buffer 2) packet drops through channel noise and interference, especially slow fading and 3) corrupted packets that were received but affected by Gilbert-Elliott channel noise to the extent that they could not be immediately reconstructed without an ARQ triggered retransmission. The Raptor code equation (1) was applied to decide if a packet could be recovered, given the number of bytes that were declared to be in error.

In the adaptive scheme, the probability of channel byte loss (*PL*) serves to predict the additional data that is piggybacked onto the next packet to be transmitted (*extra redundant data to recover packet X* in Fig. 3). Empirical investigation showed that there was insufficient provision unless approximately 10% extra data were added over and above that allowed for by a direct use of the *PL*. Moreover, this adjustment varies according to channel conditions, though the change monotonically increases according to

PL. On-going investigations seek a relationship between *PL* and the adjustment factor, *A*. If the original packet length is *L*, then the redundant data is given simply by

$$E = L \times PL \times A \quad (2)$$

when $A = 1.11$ in the evaluation experiments. Notice that the adjustment factor must also account for the full length of the packet, not just its original length.

In addition, because the *PL* derived in a simulation assumes perfect channel knowledge, which is not possible through signal strength estimation, the effect of measurement noise was modeled. A zero-mean truncated Gaussian distribution was assumed to model additive measurement noise up to a given percentage. The effect of an imperfect estimate is considered in Section V, specifically in Table V.

In fact, an estimate of channel conditions is available under WiMAX. The WiMAX standard already specifies [18] that a subscriber station should provide channel measurements that can form a basis for channel quality estimates. These are either Received Signal Strength Indicators or may be Carrier-to-Noise-and Interference Ratio measurements made over modulated carrier preambles.

V. EVALUATION

Experiments initially determined the effect of changing the percentage of redundant rateless data or alternatively adopting the adaptive scheme. In these experiments, perfect channel knowledge is assumed. No packet drops through channel conditions occur as this component of the channel model was turned off though packet corruption is certainly turned on. Thus fast but not slow fading is modeled. To judge the effect of congestion a small buffer size of five packets was set. From the discussion in Section II.A, 5% intra-refresh MBs were included. The WiMAX TDD size is fixed at 5 ms.

A fixed value for the redundant data percentage of 10% (equivalent to $\varepsilon = 0.1$ in Section II.B) was used in [19] in an Internet application, rather than this paper's adaptive scheme of Section IV. In Table IV, it is apparent that increasing the redundancy from 5% to 10% and then to the adaptive scheme of Section IV has an effect on packet drops, which impacts on video quality as FEC cannot be applied to dropped packets. Comparing corrupted packets one sees a dramatic increase in their number with only 5% redundant data but their elimination with adaptive FEC. Thus for adaptive FEC, the mean end-to-end delay of corrupted packets (the mean delay including retransmission of all corrupted packets) is zero because there are no corrupted packets. However, the reconstructed objective video quality for 5% and adaptive redundant data is much the same. There is, of course, a penalty, because the total delay in retransmitting the corrupted packets would build up if only 5% rateless coding was applied, leading to larger start-up buffers and discouraging interactive video applications. The higher percentage of dropped packets at low QP and larger packet sizes leads to unacceptable video quality, with the redundant 10% data leading to a drop in quality at QP = 25. There are small variations in the mean end-to-end packet delays, which variations are influenced by packet sizes and their propagation times. Therefore, in this set of experiments adaptive rateless coding reduces delay considerably over 5% redundant data but achieves better video quality than when using 10% redundant data. Of course, delay is an important issue in a real-time service, as it governs buffering provision, enables interactive applications, and if not checked can lead to freeze frame effects.

Table IV. Mean performance for streaming *Football* with 5%, 10% and adaptive redundant data.

	Dropped packets (%)		
QP	5%	10%	Adaptive
20	11.3	14.0	11.8
25	0	2.8	0
30	0	0	0
35	0	0	0
	Corrupted packets (%)		
QP	5%	10%	Adaptive
20	39.4	7.8	0
25	46.2	9.2	0
30	43.3	8.1	0
35	44.6	9.5	0
	PSNR (dB)		
QP	5%	10%	Adaptive
20	17.87	16.84	15.72
25	42.49	30.98	42.49
30	38.44	38.44	38.44
35	33.54	33.54	33.54
	Corrupted packet end-to-end delay (s)		
QP	5%	10%	Adaptive
20	0.0233	0.0243	0
25	0.0200	0.0203	0
30	0.0183	0.0183	0
35	0.0171	0.0171	0
	Packet end-to-end delay (s)		
QP	5%	10%	Adaptive
20	0.0127	0.0127	0.0122
25	0.0100	0.0099	0.0100
30	0.0083	0.0084	0.0083
35	0.0071	0.0071	0.0071

Table V shows the effect of including increasing percentages of measurement noise in the adaptive scheme's estimate of PL in equation (2). The main effect is that the percentage of corrupted packets increases, i.e. the percentage of packets for which a retransmission is required increases. This will have some effect on overall delay but the impact is small compared to when 5% redundant data is used. With 5% measurement noise the packet sizes for the adaptive scheme still lead to an advantage in PSNR at QP=25 over fixed 10% redundant data. Table VI now accounts for the possibility of dropped packets over the WiMAX channel. 2% additive Gaussian measurement noise

Table V. Mean performance for streaming *Football* with no channel dropped packets and varying measurement noise percentages with adaptive redundant data.

	Dropped packets (%)		
QP	2%	5%	7%
20	11.5	11.9	11.4
25	0	0	0
30	0	0	0
35	0	0	0
	Corrupted packets (%)		
QP	2%	5%	7%
20	4.6	9.7	14.6
25	4.0	12.4	18.8
30	3.7	10.8	18.6
35	1.6	9.2	15.0
	PSNR (dB)		
QP	2%	5%	7%
20	18.56	17.66	18.28
25	42.49	42.49	42.49
30	38.44	38.44	38.44
35	33.54	33.54	33.54
	Corrupted packet end-to-end delay (s)		
QP	2%	5%	10%
20	0.023	0.023	0.024
25	0.020	0.020	0.020
30	0.018	0.019	0.018
35	0.017	0.017	0.017
	Packet end-to-end delay (s)		
QP	2%	5%	10%
20	0.0122	0.0160	0.024
25	0.0100	0.0146	0.020
30	0.0083	0.0131	0.018
35	0.0071	0.0120	0.017

is set in the adaptive scheme simulation. In this set of experiments, the buffer size was set to fifty packets, effectively eliminating dropped packets arising from buffer overflow. The slice size has also been varied. Previous results assumed a single slice per picture but a wide variety of slicing arrangements are available with H.264/AVC. In the double slice option in Table VI, a picture is horizontally split into two using simple geometrical slicing. Within each slice, a separate set of DP partitions forms independent packets. Thus, the effect of slicing is to further decrease the packet sizes.

The dropping of packets now leads to unacceptable video quality when single slices are used. The quality drops below 25 dB (PSNR) which is approximately the same threshold for the ITU P.800's [20] 'fair' subjective mean opinion score rating. There is some gain in a reduction in corrupted packets and delay, but the main gain from reduction in packet size is the reduction in channel packet drops.

The gain from choosing an appropriate value of QP for DP and in general selecting smaller packet sizes is illustrated by Table VII. Table VII is an analysis of the packet (channel) drops of the results in Table VI. In the single slice results, the number of packet drops is arranged in reverse order of partition priority for lower QPs. Provided the percentage of intra-refresh MBs is restricted then the

Table VI. Mean performance for streaming *Football* with no channel dropped packets, 5% measurement noise and different slicing.

	Dropped packets (%)	
QP	Single slice	Double slice
20	6.53	2.62
25	3.46	2.69
30	3.20	1.86
35	2.05	1.09
	Corrupted packets (%)	
QP	Single slice	Double slice
20	11.79	11.36
25	12.69	10.27
30	11.15	10.14
35	8.33	6.42
	PSNR (dB)	
QP	Single slice	Double slice
20	18.03	30.29
25	21.28	20.62
30	24.76	31.03
35	23.39	26.43
	Corrupted packet end-to-end delay (s)	
QP	Single slice	Double slice
20	0.023	0.014
25	0.020	0.013
30	0.019	0.012
35	0.017	0.011
	Packet end-to-end delay (s)	
QP	Single slice	Double slice
20	0.0123	0.0091
25	0.0098	0.0075
30	0.0082	0.0068
35	0.0070	0.0061

Table VII. Number of dropped packets when streaming *Football*.

	No. of dropped NALUs		
	Single slice		
QP	Partition-A	Partition-B	Partition-C
20	13	15	24
25	4	11	12
30	7	10	8
35	5	6	5
	Double slice		
QP	Partition-A	Partition-B	Partition-C
20	5	11	28
25	9	14	19
30	11	9	9
35	10	5	2

partition-B packets are kept small in size and its losses are small. However, there is not a direct relationship between packet drop numbers and mean packet size, as in Table II partition-B bearing packets tend to be smaller than those of partition-A, yet more partition-B single slice packets are dropped.

For higher QPs, when the relative size of partition-A and -B bearing packets increases, there is no advantage given to the higher-priority partition packets. Similar relationships hold for the double slice results. However, as there is now double the number of packets, the percentage of packets dropped out of the total is actually much lower. An interesting feature of these results is that relative size across the DP packets has an impact on packet drops. The gain from packet size differentiation across the partitions was

more stark for Table IV's packet drops from congestion for QP = 20. No partition-A bearing packets were lost, whereas for 2% measurement noise 21 partition-B packets and 69 partition-C packets were dropped. Similar results occurred for the higher percentages of measurement noise. However, as it turned out the level of packet drops at QP = 20 were such as to have no practical impact, as video quality fell below the threshold of acceptability.

Though space does not permit inclusion of the results, we have conducted similar experiments with the reference *Paris* sequence with the same encoding format as for *Football*. *Paris* is a longer sequence (1065 frames) with two presenters in a TV studio. Motion is moderate but the background has high spatial coding complexity. Though quality of experience tests show [21] that mobile users favor this type of clip, *Football* is more challenging to transmit. The tests for *Paris* showed similar trends as for Football but the video quality outcomes were better because the impact of packet loss is not so large.

VI. CONCLUSION

Layered video-coding through DP video allows the relative packet sizes across the partition types to be manipulated by selection of the QP. Broadly high quality video with QP at 20 fared badly in experiments because the larger packet sizes left the video stream vulnerable to drops either from buffer overflow due to traffic congestion or to adverse channel conditions, typically arising from deep fades. Higher QPs and lower video quality increases the relative size of partition-A packets, again leading to poorer video quality. Therefore, medium quality video streams may be best suited to streaming with DP video. A complicating factor is the use of intra-refresh MBs because the inclusion of these MBs changes the relative sizes of partition-B and partition-A packets. Though reception of partition-A packets is vital, partition-B packets then contribute to the cancellation of temporal error propagation. The advantage of adaptive rateless coding was demonstrated in this paper. However, in terms of DP video, this is an equal error protection scheme. Packet size is certainly important in protecting against packet drops before FEC can even be applied. However, an unequal error protection scheme that also preserved the advantage of relatively smaller packet sizes may be attractive. Ongoing work is investigating the use of redundant partition-A packets. This could simply be replicating the original partition-A packets but this increases the bit rate. Therefore, the size of the redundant partition-A packets can be reduced by raising the QP.

REFERENCES

[1] A. H. Li, S. Kittitornkun, Y. H. Hu, D. S. Park, and J.D. Villasenor, "Data partitioning and reversible variable length codes for robust video communications," *In Proc. of Data Compression Conf*., Snowbird, UT, USA, pp. 460-489, May 2002.

[2] M. Ghanbari, "Layered video coding," in M.T. Sun and A. Reibman (ed.), *Compressed Video over Networks*, Marcel Dekker, Inc., 2000.

[3] "BBC iPlayer growth continues as bbc.co.uk records 29% increase," Feb. 2008 [Online] Available: http://www.bc.co.uk/pressoffice/ pressrelease/stories/2008/02.february/

[4] J.M. Lee, H.-J. Park, S. G. Choi, and J. K. Choi, "Adaptive hybrid transmission mechanism for on-demand mobile IPTV over WiMAX," *IEEE Trans. Broadcasting*, vol. 55, no.2, pp. 468-477, 2009.

[5] IEEE, 802.16e-2005, IEEE Standard for Local and Metropolitan Area Networks. Part 16: Air Interface for Fixed and Mobile Broadband Wireless Access Systems, 2005.

[6] T. Wiegand, T. Noblet, and F. Roblati, "Scalable video coding for IPTV services," *IEEE Trans. Broadcasting*, vol. 55, no.2, pp. 527-538, 2009.

[7] L.-A. Larzon, M. Degermark, S. Pink, L.-E. Jonsson, and G. Fairhurst, "The lightweight user datagram protocol (UDP-Lite)," IETF, RFC 3828, Jul. 2004.

[8] D. J. C. MacKay, "Fountain codes," *IEE Proc.: Communications*, vol. 152, no. 6, pp. 1062–1068, 2005.

[9] Effnet AB, "An introducton to IP header compression," White Paper, Bromma, Sweden, Feb. 2004.

[10] B. Barmada, M. M. Mahdi, E. V. Jones, and M. Ghanbari, "Prioritised transmission of data-partitioned H.264 video with hierarchical QAM," *IEEE Sig. Proc. Letter*, vol. 12, no. 8, pp. 577-580, 2005.

[11] R.M. Schreier, and A. Rothermel, "Motion adaptive intra refresh for the H.264 video coding standard," *IEEE Trans. Consumer Electronics*, vol. 52, no. 1, pp. 249- 253, 2006.

[12] T. Wiegand, G. J. Sullivan, G. Bjontegaard, and A. Luthra, "Overview of the H.264/AVC video coding standard," *IEEE Trans. Circuits Syst. Video Technol.*, vol. 13, no. 7, pp. 560-576, July 2003.

[13] A. Shokorallahi, "Raptor codes," *IEEE Trans. Information Theory*, vol. 52, no. 6, pp. 2551-2567, 2006.

[14] M. Luby, T. Gasiba, T. Stockhammer, and M. Watson, "Reliable multimedia download delivery in cellular broadcast networks," *IEEE Trans. Broadcasting*, vol. 53, no. 1, pp. 235-246, 2007.

[15] F. C. D. Tsai, et al., "The design and implementation of WiMAX module for ns-2 simulator," *Workshop on ns2: the IP network simulator*, article no. 5, 2006.

[16] G. Haßlinger and O. Hohlfeld, "The Gilbert-Elliott model for packet loss in real time services on the Internet," in 14th GI/ITG Conf. on Measurement, Modelling, and Evaluation of Computer and Commun. Systs., pp. 269-283, 2008.

[17] J. Klaue, B. Rathke, and A.Wolisz, "EvalVid - A framework for video transmission and quality evaluation," *In Proc. Int'l Conf. on Modeling Techniques and Tools for Computer Performance*, 2003, pp. 255-272.

[18] L. Nuaymi, *WiMAX: Technology for Broadband Wireless Access*, J. Wiley & Sons Ltd, Chichester, UK, 2007.

[19] S. Ahmad, R. Hamzaoui, M. Al-Akaidi, "Robust live unicast video streaming with rateless codes", *In Proc. Int'l PacketVideo Workshop*, Nov. 2007.

[20] ITU-T Rec. P.800 Methods for subjective testing of video quality, 1996.

[21] F. Agboma and A. Liotta, "Addressing user expectations in mobile content delivery," *Mobile Information Systems*, vol. 3, no. 3/4, pp. 153–164, 2007.